Thermoelectric Films – Potential for new miniaturized Devices

Matthias Stordeur and Guido Willers
angaris GmbH
Heinrich-Damerow-Straße 1, D-06120 Halle, Germany
Matthias.Stordeur@angaris.de, Phone: +49 345 27 99 64 50, fax: +49 345 27 99 64 51

Abstract

In the last decade thermoelectric films were under continuously basic and applied investigations finally with the target to develop new thermoelectric devices including the corresponding technology for special and volume applications in form of miniaturized Peltier coolers and thermoelectric generators.

To characterize the reached level and chances for future device developments it is useful to classify the films of thermoelectric materials in three groups:

i. homogeneous thermoelectric films with a thickness in the range of about 1 µm ... 30 µm, showing no special significant physical effects compared with the corresponding bulk materials
ii. periodical (in 10 nm range) non-uniform thin (a few µm) thermoelectric films form a 2-dimensional charge carrier gas (2DEG) with drastically changed electronic properties caused by quantum confinement in the plane normal to the growth direction
iii. superlattices layer structures for the reduction of the phonon thermal conductivity without a deterioration of the electronic material properties; phonon-blocking / electron-transmitting

Whereas thermoelectric films of the group (i) can be designed for devices in the in-plane and in the cross-plane arrangement, to use the enhanced 2DEG-values of the thermoelectric figure-of-merit Z for the group-(ii)-films only an in-plane transport seems meaningful. For the case (iii) the reduction of the phonon thermal conductivity appears predominantly for cross-plane fluxes and rises Z in this direction for a favorably using in miniaturized devices.

A review is given about the advantages and disadvantages of the different film device concepts including technological aspects as e. g. film deposition, pattern generation and micro assembling. The influences of the figure-of-merit, the power factor and the thermal and electrical contact resistances on the device parameters are discussed.

Bi_2Te_3-type material films stand in the focus of attention, but also silicon based and other thin film devices will be mentioned.

Introduction

Thermoelectric devices based on compact polycrystalline or sintered materials are state of the art and world-wide well established products as generators or solid state coolers using the Seebeck or Peltier effect, respectively, for the direct energy conversion of heat into electricity and vice versa (see e. g. [1, 2]).

The development efforts during the recent years have been led to a drastically reduction of energy consumption for micro and sensor systems as well as for opto-electronic components. In the last decade this progress has stimulated the miniaturization of thermoelectric devices especially by the application of functionally materials in form of films [3, 4, 5] to meet the requirements of such low power loads. Films mean here layers (or wires), which were not generated by cutting or sawing of compact bulk materials.

A wide range of technologies have been developed in the last years to prepare such thermoelectric films as e. g. magnetron sputtering [3,4,5,6], electrochemical deposition (plating) [7, 8, 9], laser ablation [10, 11], co-evaporation [12], printed by using micro-jet [13], and others. The motivation of these broad recent activities has been given for various reasons, so the improvement of the thermoelectric properties of the films in comparison with the corresponding bulk materials and the possibility to design miniaturized devices by using of such films. The first aspect is the subject of detailed investigations including theoretical modeling of the electrical conductivity σ, the Seebeck coefficient S, and the thermal conductivity κ, which form the figure-of-merit Z and the power factor P, as the central magnitudes for the quantitative description of the quality of thermoelectric materials:

$$Z = S^2\sigma/\kappa = P/\kappa \qquad (1)$$

For prototyping of thermoelectric film devices in addition to the deposition methods the control of the pattern generation (p-legs, n-legs, contacts) is very important. In combination with a photolithographic process wet chemical etching [3, 4], plasma dry etching [5], or the use of templates [7, 12] are chosen procedures for film structurization. Finally a micro assembling is required for a complete device construction [4, 5, 7].

Whereas the active (room temperature) thermoelectric films presented in [3, 5, 7, 12] consist of V_2VI_3-semiconductors, most as alloys of the compounds Bi_2Te_3, Sb_2Te_3, and Bi_2Se_3 with dopands and / or excesses, also poly-Si / poly-$Si_{70}Ge_{30}$ [14] and doped poly-Si / Al [15, 16] thin film thermocouples are used for thermoelectric generators and sensors.

For miniaturized low power thermoelectric generators there are wide application fields as self-powered energy sources. One segment is to convert body heat from humans or animals into electrical energy to supply wearable electronics, so e. g. electronic wrist watches, medical sensors to detect blood pressure, pulse frequency or body temperature as well as tracking or sports sensors (distance, velocity). If a living organism is in the role of the heat source, only relatively small temperature differences (about 5 K) are useable. Whereas by using of general waste heat we can find sometimes also small temperature differences but in a few cases the difference is distinct larger in the order of a few 10 K. Examples for waste heat conversion are electronic heat cost allocators, electronic heat meters, warm and cold water meters, active transponders or self-powered wireless temperature control systems. A relatively new application trend for low power thermoelectric

generators is in the automotive industry as decentralized power supply for electronics and sensors (e. g. oil pressure and level, water temperature) within the motor management system. This saves leads, mass and energy in the motor vehicle.

Also as Peltier coolers miniaturized film thermoelectric devices become increasing interested for keeping laser diodes or other solid state light emitters at the right temperature [17].

Nevertheless, whereas a broad type-spectrum of bulk-material Peltier coolers and also power generators are commercial available on the international market, film generators are still in the stage of prototyping (exception: thermopile sensors) and yet far from a volume production. Two reasons seem to be responsible for this fact. At first there are still a lot of technological problems, which are under the investigation at the present time but are not complete solved satisfactory concerning the aspects of productivity and costs. And second it is to recognize that the fact to produce electrical energy by the generators alone does not lead to the substitution of the relative low priced and also long life electrochemical batteries or other conventional energy stores. Further advantages of the thermoelectric generators have to come in addition to meet a decision for the application of this innovative device, as e. g. high reliability, no maintenance, no battery change, true long life stand-alone solutions, energy recycling of waste heat, environment kindly.

In the following we will try to give a survey about the development stage of thermoelectric film devices with the goal to sharpen the view to the activities, which have to be done these components to make fit for the market.

Classification

Thermoelectric film devices are suitable as generators or coolers for low power applications finally caused by their small volume of the active materials. Like in the case of bulk devices there is not an all-round film device for all applications in its performance category. A careful analysis of the heat and energy balances of the special application prior the employment can provide for a perfectly matched design of the device.

Partly supported by the governments and industries in addition to basic research currently strong efforts have been made for prototyping of film devices generated by different materials, with various film deposition and pattern generation technologies, mainly in two different geometrical configurations by using of "normal" transport properties [4, 5, 17, 18], under the specific conditions of quantum confinement [19, 20, 21] or by transport through superlattices [22, 23].

In-plane and cross-plane configurations

At first we consider the both different geometrical device arrangements so called in-plane and cross-plane configurations shown schematically in Fig. 1 and Fig. 2, respectively.

There is a big diversity to design the in-plane configuration (see Fig. 1) especially for power generation. For an useable power output the thermoelectric active films have a thickness in the order of at least a few microns. The p- and n-legs with the typical length in the mm-range are mechanical supported by a necessary substrate, which can be e. g. a polyimid foil as in the case for V_2VI_3-materials [4] or a freestanding membrane by using of CMOS-compatible technologies [14, 24]. Besides electrical insulation, a film-matched thermal expansion coefficient, a sufficient solidity and a good adhesive interface, the substrate have to be distinguished by a small thermal conductivity in relation to the semiconductor materials.

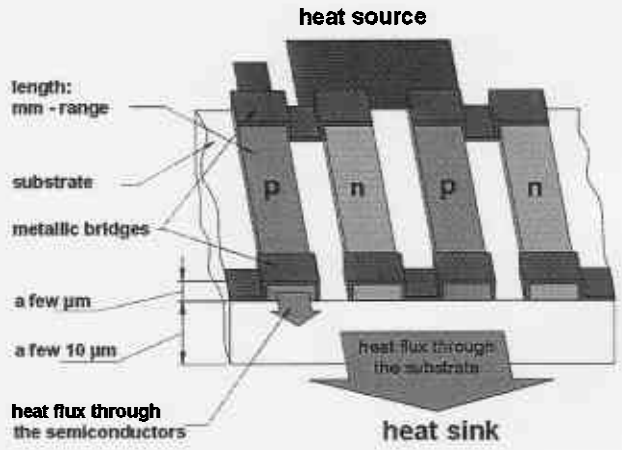

Advantages

- relatively high voltages already at small temperature differences
- frequent adequate power output for a lot of applications
- Mainly the power factor of the TE-materials determines the electrical device parameter.
- Film thickness in the a few µm range requires only a relatively short deposition time.
- relatively small heat flux
- Electrical contact resistance does not play an important role.
- relatively small thermo-mechanical stress by small temperature gradients

Disadvantages

- small efficiency caused by parasitic heat flux through the substrate
- high internal electrical resistance by small leg cross sections
- relatively high expenditure for micro assembling

Fig. 1: In-plane device arrangement (schematic, with short characterization)

Nevertheless the parasitic heat flux through this substrate is an essential disadvantage of the in-plane configuration. But in spite of these thermal losses this arrangement shows also a series of advantages (see list in Fig. 1) especially concerning its electrical behavior. By stacking on top of one another of such thin film segments (see Fig. 1) in a micro assembling procedure miniaturized generators can be fabricated with a few thousand thermocouples in series.

The in-plane configuration of the film thermopiles is also the favorable structure for sensor designs as contact less temperature sensor (ir-detectors) [4, 25], flux meters for gases and liquids [15, 26, 27], chemo- and biosensors and micro calo-

rimeters by detection of reaction heats [28] as well as for high frequency power detectors [29].

The alternative to in-plane is the cross-plane configuration, see Fig. 2. This arrangement is corresponding to the standard Peltier coolers only with extremely short legs in form of a few 10 µm thick thermoelectric films. The substrate in the cross-plane configuration also acts as heat couple plates for the device connection with the heat source and sink. The substrate thickness is here about ten times larger than the film-leg lengths. To minimize losses of the temperature differences the substrate material should have a high thermal conductivity, so as diamond, AlN-, BeO-, Al_3O_3-ceramics but also Si.

It is a well-known fact that shorter leg lengths lead in the tendency to a drastic enhancement of the cooling power. But in the reality this increase is limited by rising electrical and thermal losses due to the increasing influence of the electrical and thermal contact resistances. More detailed quantitative estimations to this subject are given in [2].

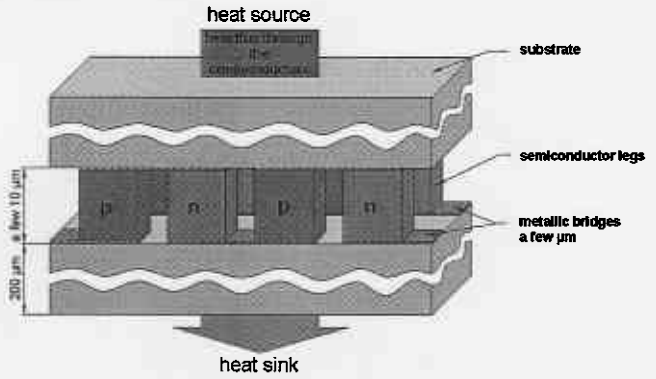

Advantages

- relatively high power output already at small temperature differences
- relatively high efficiency
- heat flux only through thermo-legs, no parasitic
- small internal electrical resistance by short legs

Disadvantages

- Film thickness in a few 10 µm range requires a relatively long deposition time.
- Electrical and thermal contact resistances play an important role.
- relatively high heat flux by a small thermal resistance
- relatively strong thermo-mechanical stress by high temperature gradients

Fig. 2 Cross-plane device arrangement (schematic, with short characterization)

Further features of the cross-plane configuration are collected in Fig. 2. At a typical sputter rate of about 1 nm/s for the deposition of thermoelectric semiconductors the growing of a 10 µm film lasts about 2.5 h. It seems that the disadvantages of the cross-plane configuration appears stronger in the Peltier mode than the device works as generator. Nevertheless to guarantee a possible high temperature difference in spite of relative strong heat fluxes, it is a sophisticate task to meet all requirements for the heat exchange system especially on the cold side.

Film materials: "normal" films

The bulk materials with the highest figure-of-merit Z (see (1)) have often also in form of films the best thermoelectric properties. At first we will consider "normal" films those transport behavior is determined by the charge carrier gas, filling the 3-dimensional space. That means in these films the same electronic band structure is shown as in the corresponding compact crystals, also analogous charge carrier and phonon scattering processes act than in the bulk materials often added by grain boundary scattering which is typical for polycrystalline films.

Whereas for the optimization of film devices in the cross-plane configuration all criteria valid for the conventional Peltier coolers and generators including the contact resistances (see e. g. [30]) are applied and the figure-of-merit of the used materials plays the central role, at the in-plane arrangement the power factor (see (1)) comes to the fore due to the parallel parasitic heat flux through the substrate.

At the draft of a thermoelectric film device matched to application specific requirements, the selection of the active materials plays an important role. Often the main criterion for the material choice is the working temperature of the device. Under this aspect we resort to the well-known dependence of the bulk figure-of-merit Z of the temperature, demonstrated in Fig. 3 after [31].

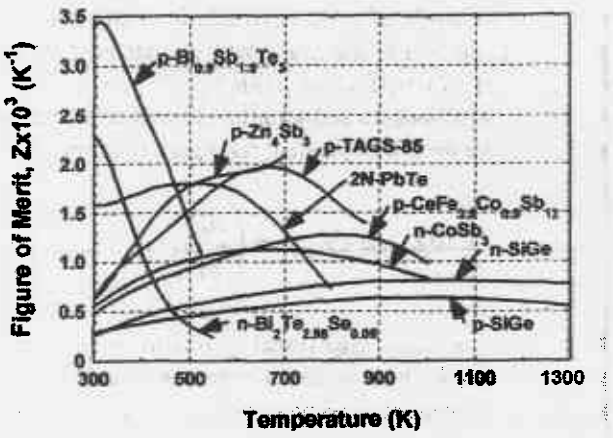

Fig. 3: Dependence of the figure-of-merit of the temperature for typical thermoelectric bulk materials after [31]

Standard materials of Bi_2Te_3-type alloys have the highest figure-of-merit Z around room temperature, followed by IVVI-compounds as PbTe or $PbSn_xTe_{1-x}$, $(AgSbTe)_{1-x}(GeTe)_x$ belonging to the TAGS (compounds of the elements Te, Ag, Ge, Sb), skutterudites as $CoSb_3$, and Ge/Si-alloys at higher temperatures. Of course not all known thermoelectric materials were considered in Fig. 3.

Now we remember the relationship between the usable output power N of a generator device with the intrinsic resistance R_i and the total Seebeck coefficient S ($S = S_p - S_n$, $S_n < 0$, S_p and S_n are the Seebeck coefficients of the p- and n-leg, respectively) at the temperature difference ΔT and the power factor P introduced by (1).

$$N = \frac{U_l^2}{R_l}, \quad (2)$$

where U_l is the voltage at the external load resistance R_l. U_{op} is the voltage in the open circuit and it is valid

$$U_{op} = S\Delta T \quad (3)$$

and with

$$U_l = \frac{R_l}{R_l + R_i} U_{op} \quad (4)$$

we define $\mu = R_l/R_i$ as the ration of the load to the internal resistance then follows for the power output N:

$$N(\mu) = \frac{\mu^2}{R_l(1+\mu)^2} U_{op} = \frac{\mu}{R_i(1+\mu)^2} S^2(\Delta T)^2 \quad (5)$$

From the right term in (5) we see that N reaches a maximum for $\mu = 1$, means $R_l = R_i$:

$$N_{max} = \frac{S^2(\Delta T)^2}{4R_i} (\propto S^2\sigma = P) \quad (6)$$

The proportionality in (6) is then valid if the p- and n-legs ($\sigma = \sigma_n + \sigma_p$) have the same length and cross section and the electrical contact resistances are small in relation to the path resistance of the thermoelectric films. The last-mentioned fact is mostly correct for the in-plane configuration (see Fig. 1) and less correct for the cross-plane arrangement (see Fig. 2). Nevertheless based on eq. (6) we can cautiously formulate, that an enhancement of the power factor leads to a rising of the generator output power. Of course the assumption is here, that the optimization procedure of the power factor does not cause an essentially change (increase) of the thermal conductivity.

In the case of material films it seems to be useful to consider the power factor a little bit separately besides the figure-of-merit. So as an example the power factors as bulk or film property of p- and n-type Bi_2Te_3-materials are listed in Table 1.

The Seebeck coefficient and the electrical conductivity of the films are not only determined by the selected composition but also can be influenced by a series of further growth conditions as e. g. the deposition method, kind of substrate (glass, mica, BaF_2, silicon, polyimid), substrate temperature, and thermal post treatment. But if we evaluate the power factor values given in Tab. 1 in the tendency we come to the following conclusions.

For p- and n-Bi_2Te_3-type single crystals the power factors have equally the highest values compared with the corresponding sintered and film materials. The power factors of sintered materials reach nearly the values valid for the single crystals, whereas the film power factors as well as for the p- and n-type semiconductors are distinctly smaller. But we recognize also differences between the p- and n-system at the comparison between the transport properties of the bulk and film modification. As the best single crystal power factor for p-$(Bi_{0.25}Sb_{0.75})_2Te_3$ was found to 45 $\mu W/(cmK^2)$ and the highest film value for the very similar composition p-$(Bi_{0.15}Sb_{0.85})_2Te_3$ is given by 38 $\mu W/(cmK^2)$. That means in the p-system the film power factor is about 15 % smaller than the bulk ones. On the other hand in the n-system the differences between the bulk and film parameters are essentially larger near 26 %, indicated by 52 $\mu W/(cmK^2)$ for the n-$Bi_2(Te_{0.95}Se_{0.05})_3$ bulk power factor and 40 $\mu W/(cmK^2)$ [36] for the n-Bi_2Te_3 film value, which seems already to be exceptional high compared with other n-film data [17] (see Tab. 1). Therefore for the enhancement of the power output (see (6)) of thin film generators using V_2VI_3-materials it is a currently task of prime importance to improve the power factor of the n-semiconductor layers. That means in the first line it have to be achieve an increasing of the electrical conductivity, because this quantity is stronger negatively influenced by the grain boundary scattering than the Seebeck coefficient.

Table 1: Power factors (max.) of p- and n-Bi_2Te_3-type-materials near room temperature (c – trigonal axis)

Type	Composition	Form	Power factor $\mu W/(cmK^2)$	Remarks	Ref.
p	$(Bi_{.25}Sb_{.75})_2Te_3$	bulk	45	single crystal, $\perp c$	[32]
p	$(Bi_{.25}Sb_{.75})_2Te_3$	bulk	38, 41	sintered	[33, 34]
p	$(Bi_{.25}Sb_{.75})_2Te_3$	bulk	42	extrusion	[35]
p	$(Bi_{.15}Sb_{.85})_2Te_3$	film	36	sputtered, annealed	here
p	$(Bi,Sb)_2Te_3$	film	30	sputtered, annealed	[17]
p	$(Bi_{.15}Sb_{.85})_2Te_3$	film	38	sputtered, annealed	[6]
p	Sb_2Te_3	film	28	co-evaporation	[36]
n	$Bi_2(Te_{.95}Se_{.05})_3$	bulk	52	single crystal, $\perp c$	[37]
n	$Bi_2(Te_{.95}Se_{.05})_3$	bulk	30, 32	sintered	[38, 39]
n	Bi_2Te_3	film	16	sputtered, annealed	[17]
n	$Bi_2(Te_{.9}Se_{.1})_3$	film	10-13	sputtered, annealed	here
n	Bi_2Te_3	film	40	co-evaporation	[36]

Power factors are also available for n-Bi_2Te_3 and p-Sb_2Te_3 prepared by co-evaporation of powder of the corresponding elements onto a SiO_2-insulating silicon wafer as substrate. Compared with other investigations (see Tab. 1) the maximum values given in [12] with 2.9 $\mu W/(cmK^2)$ for n-Bi_2Te_3 and 7.6 $\mu W/(cmK^2)$ for p-Sb_2Te_3 are relatively small.

Now we look at the dependence of the electrical transport properties of the temperature for sputtered and annealed p- and n-type V_2VI_3-films. For p-$(Bi_{0.15}Sb_{0.85})_2Te_3$ and n-$Bi_2(Te_{0.9}Se_{0.1})_3$ the conductivity σ, the Seebeck coefficient S and the power factor P are presented in Fig. 4 and Fig. 5, respectively. The p-film was deposited onto a polyimid foil with a thickness of 75 µm and formed a 1 µm thick layer. With the aim to reduce the parasitic heat fluxes through the substrate for in-plane applications (see Fig. 1) the n-film with a thickness of 6.4 µm was sputter-deposited onto a thinner 25 µm-polyimid foil also for mechanical testing of film-substrate compound under thermal stress.

To have a comparison the measurements were carried out by using of two apparatus (app. 1, app. 2 in Figs. 4 and 5). The first equipment was only able to measure σ and S near room temperature at max. 90 °C. In this case gluing or soldering direct on the film or on especially metallic contacts realized the required contacts. The second measuring apparatus was working over a wide temperature range (about 5 K to 1000 K) under vacuum or inert gas atmosphere. For the registration of the electric voltages the film sample was connected with pressure contacts. For controlling of the film homogenei-

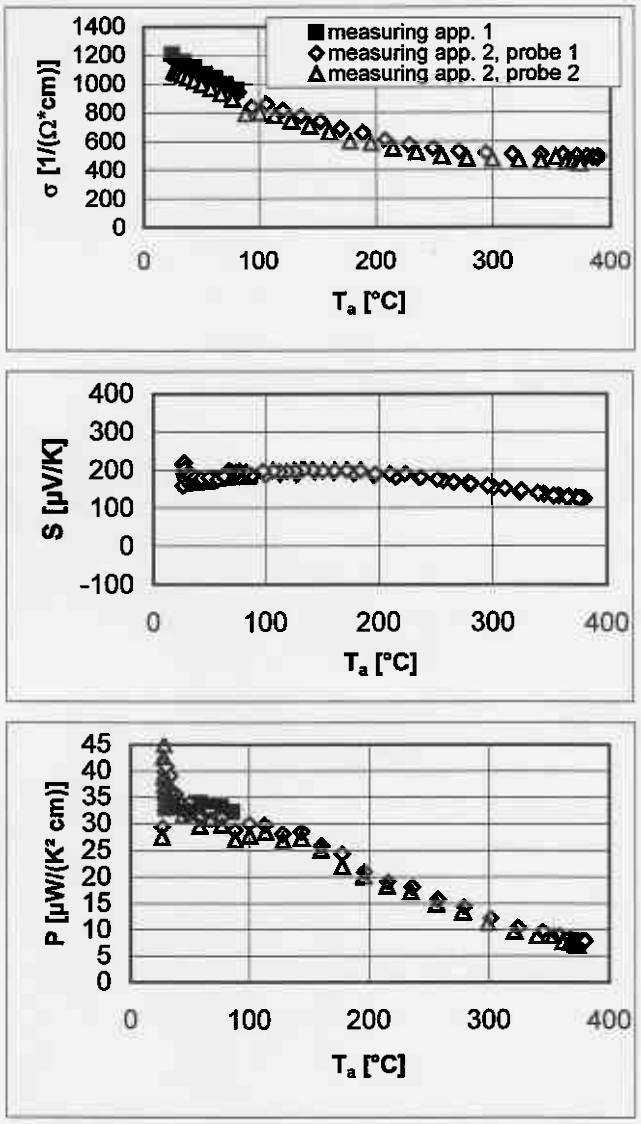

Fig. 4: Dependence of the electrical conductivity σ, the Seebeck coefficient S and the power factor P of the average temperature T_a for a p-$(Bi_{0.15}Sb_{0.85})_2Te_3$ sample (sputtered, annealed, thickness 1 µm, substrate: 75 µm polyimid; insert: see text)

ty and the absence of macroscopic imperfections as e. g. mechanical cracks the second equipment allows to measure the ohmic drop in voltage and the thermo voltages between two probe pairs (probe 1 and 2 in Fig. 4), distinguished by different distances of the contacts.

The electrical conductivity of the p-$(Bi_{0.15}Sb_{0.85})_2Te_3$ film decreases monotonously from about 1200 $(\Omega cm)^{-1}$ at room temperature to about 500 $(\Omega cm)^{-1}$ at 400 °C (see Fig. 4). Obviously up to this temperature the intrinsic carrier generation does not play a measurable role. The measurement results for probe1 and probe 2 are about the same within the experimental error. That speaks for a good thermo mechanical stability of the film-foil compound under the considerable thermal stress up to 400 °C. In addition we establish that as well as for the electrical conductivity and the Seebeck coefficient the values for the p-film (see Fig. 4) measured with apparatus 1

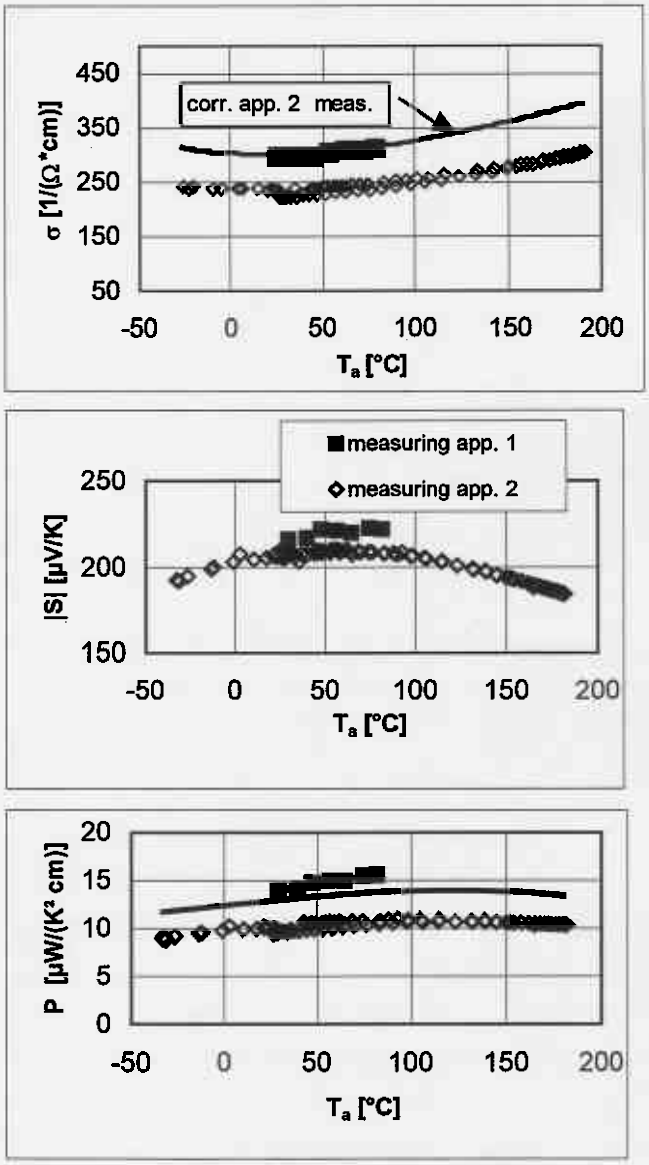

Fig. 5: Dependence of the electrical conductivity σ, the Seebeck coefficient S and the power factor P of the average temperature T_a for a n-$Bi_2(Te_{0.9}Se_{0.1})_3$ sample (sputtered, annealed, thickness 6.4 µm, substrate: 25 µm polyimid; insert: see text)

and apparatus 2 are almost identical.

From room temperature up to 250 °C the p-Seebeck coefficient is about 190 µV/K and does not change. For higher temperatures S decreases up to about 120 µV/K (see Fig. 4).

This could be related with the beginning influence of the intrinsic conduction on the Seebeck coefficient.

As consequence of the behaviour of $\sigma(T)$ and $S(T)$ the power factor for the p-$(Bi_{0.15}Sb_{0.85})_2Te_3$ film decreases with rising temperature.

Analogous measurements were carried out for n-$Bi_2(Te_{0.9}Se_{0.1})_3$ films in the temperature range from –30 °C to 180 °C (see Fig. 5). Near 75 °C an increase of the electrical conductivity and a decrease of the Seebeck coefficient as a consequence of the beginning intrinsic conduction have been observed. This leads for the n-film to a power factor, which is nearly independent of the temperature in this range.

Differently from the results of the p-film sample differences mainly of the electrical conductivity appeared between the measurements with apparatus 1 and apparatus 2 with the values of 300 $(\Omega cm)^{-1}$ and 230 $(\Omega cm)^{-1}$ near room temperature, respectively. Probably this discrepancy was caused by mechanical micro damages in the more sensitive n-film-foil compound from the pressure contact used in apparatus 2. Therefore the data determined in apparatus 2 over the whole temperature range was corrected based on the values measured in apparatus 1 near room temperature. This leads there to an enhancement of the power factor from 10 $\mu W/(cmK^2)$ to 13 $\mu W/(cmK^2)$.

Although the power factors of the V_2VI_3-films decrease (p-type) or keep almost unchanged (n-type) with rising temperature (Figs. 4 and 5) their values near 200 °C lie in the same order as for PbTe-films and are distinct higher as e. g. for MnSi- or $FeSi_2$-films [40]. From material properties point of view "normal" V_2VI_3-films can be used for devices up to a working temperature of about 200 °C and represent here an alternative for PbTe-layers.

It is well known, that the figure-of-merit of SiGe-alloys is relatively high at high temperatures (see Fig. 3) in comparison with other thermoelectric materials, but near room temperature there are compounds with more suitable properties for applications especially for thermoelectric micro generators. This is also applied to the power factors of these alloys, which are given near room temperature in [41] e. g. for polycrystalline p- and n-$Si_{0.8}Ge_{0.2}$-films with 1.4 $\mu W/(cmK^2)$ and 3.6 $\mu W/(cmK^2)$, respectively.

Film materials: multiple quantum wells and superlattices

In early papers [19, 20, 21] were predicted and in first experiments also confirmed, that the thermoelectric figure-of-merit can be considerably enhanced, if the quasi free move-

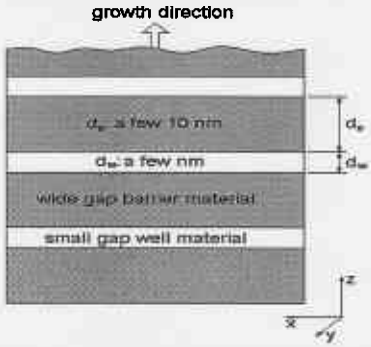

Fig. 6: Multiple quantum well (MQW) structure (schematically)

ment of electrons or holes is limited on two dimensions, the carriers form a two dimensional electron gas (2DEG). Systems, which such transport conditions, can be created artificially by alternating layer stacking of a wide gap and a small gap material. The wide gap material is in the role of a barrier layer with the thickness d_B and the small gap semiconductor with the thickness d_W forms a quantum well for the confinement of the electron gas (2DEG). Such a multiple quantum well (MQW) structure is schematically shown in Fig. 6.

Under the simplified assumptions that the charge carriers occupy only the lowest sub-band in the quantum well with a parabolic dispersion relation, tunnelling through the barrier layer does not exist, the heat flux through the barriers is neglected and the phonon thermal conductivity of the well is the same as for the corresponding bulk material, the new quality of the thermoelectric in-plane transport (perpendicular to the growth direction) is characterized by typical features [21].

It is possible to define a two-dimensional figure-of-merit Z_{2D} given in eq. (7), where $F_i(\zeta^*)$ are the usual Fermi integrals and ζ^* is the reduced Fermi level relative to the edge of the first sub-band. The expression B_{2D} in eq. (8) contains parameters describing the material properties of the quantum well as the effective masses m_x, m_y and the mobility μ_x of the carriers.

$$Z_{2D}T = \frac{(\frac{2F_1}{F_0} - \zeta^*)^2 F_0}{\frac{1}{B_{2D}} + 3F_2 + \frac{4F_1^2}{F_0}} \tag{7}$$

$$B_{2D} = \frac{1}{2\pi d_W}(\frac{2k_BT}{\hbar^2})\frac{k_B^2T(m_xm_y)^{1/2}\mu_x}{e\kappa_{ph}} \tag{8}$$

κ_{ph} is the phonon part of the thermal conductivity, k_B the Boltzmann constant, e and $\hbar$ are the elementary charge and Planck's constant divided by 2π, respectively. In contrast to the "normal" 3-dimensional figure-of-merit Z_{3D} (see eq. (1) and explicit in [21]) Z_{2D} depends on the quantum well thickness d_W as an additional parameter. In the 2-dimensional case this opens the possibility to maximize $Z_{2D}T$ (see (7)) in two steps. The first step is the reduction of d_W, what means a decrease of $1/B_{2D}$ and in the second step for a fixed d_W, which is typical in the range from 1 nm to 6 nm, the carrier density can be varied to match an optimized reduced Fermi level ζ^* for a maximum of Z_{2D}.

In dependence of the investigated materials the enhancements of the dimensionless figure-of-merit $Z_{2D}T$ by the factor of about 2 to 10 compared to $Z_{3D}T$ was estimated in [21], but in the tendency these predictions have been established as too optimistic, caused by the too simple assumptions of the theoretical model. Theoretical considerations under more realistic assumptions were carried out in [42]. As a result Z_{2D} is limited in the case of thin wells and barriers by tunnelling of the carriers in the barriers and at thicker layers by the increasing of the thermal conductivity. An example for $Z_{2D}T$ where these effects were taken into the consideration is given in Fig. 7 after [42] for a Bi_2Te_3 superlattice. Only for thinner wells an enhancement of $Z_{2D}T$ over the bulk value can be observed and reaches a maximum. The further decrease of d_W (= a) leads to

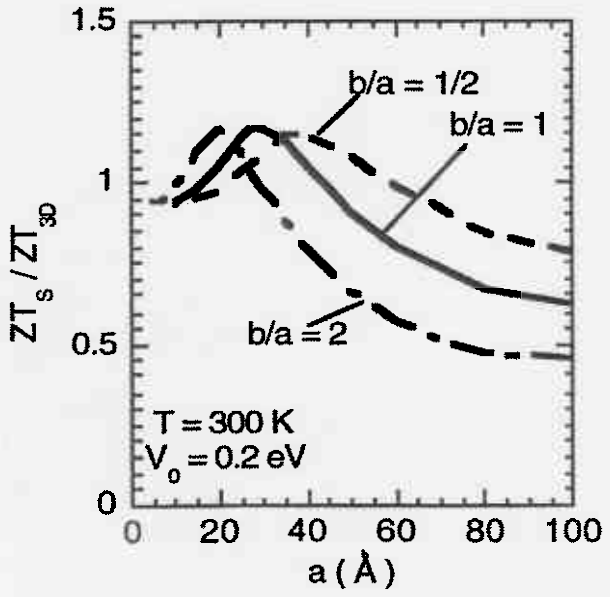

Fig. 7: The Bi_2Te_3 superlattice figure-of-merit $Z_{2D}T$ (= ZT_S) scaled by $Z_{3D}T$ (= ZT_{3D}) for the corresponding bulk material after [42] given as a function of the well width d_W (= a) for several d_B/d_W-ratios (barrier width d_B = b), d_B/d_W = ½ (dashed line), d_B/d_W = 1 (solid line), and d_B/d_W = 2 (dashed-dotted line); V_0 is the barrier height.

a reduction of $Z_{2D}T$ due to tunnel effect, for the decrease at thicker wells the rising of the thermal conductivity is responsible.

Experimental results are given in [43] for the MQW-system p-type $Pb_{1-x}Eu_xTe/PbTe$ with x = 0.073. The well layer is PbTe and $Pb_{0.927}Eu_{0.073}Te$ forms the barrier film. d_W lies near 2 nm and the barrier width d_B is about 20 nm (see Fig. 6); the total sample thickness was about 5 µm. At a temperature of 300 K for $Z_{2D}T$ the value of 1.5 was determined within the quantum well, this corresponds to $5 \cdot 10^{-3}$ K^{-1} for the 2-dimensional figure-of-merit Z_{2D}. This means a distinct enhancement of Z_{2D} in the well for this MQW-structure compared with Z_{3D} for the best bulk thermoelectric materials (see Fig. 3) in this temperature range.

This MQW-system was continuously under the investigation in the last years and the underlying theoretical model for the explanation of the high Z_{2D} well values was permanently improved by more physical details as e. g. carrier scattering on both optical and acoustical phonons, many valley band structure with anisotropic effective masses and the temperature dependences of the gaps [44].

A further example for a MQW-system is the n-type structure $Si/Si_{1-x}Ge_x$, where Si forms the well and $Si_{1-x}Ge_x$ e. g. with x = 0.7 is used as barrier material. Thermoelectric properties of this system are described in [45]. Obvious fact here is to make a difference between the 2D-power factor, which only takes into account the properties (S_W, σ_W) within the well and the 3D-power factor which includes as well as barrier and well properties ($S_{W\&B}$, $\sigma_{W\&B}$). If well and barrier are considered as an inhomogeneous unit consisting of two different conductors, than geometrical considerations lead to the relationships between individual and total quantities (σ_W, σ_B, S_W, $S_B)_{2D} \Leftrightarrow (\sigma_{W\&B}$, $S_{W\&B})_{3D}$ explicit given e. g. in [46, 47] for transport parallel to the layers. If we assume the simple case, that the barrier consists of an insulating material with $\sigma_B = 0$ then follows for the 3D-power factor

$$\left(S^2_{W\&B}\sigma_{W\&B}\right)_{3D} = \frac{S^2_W \sigma_W}{1+\frac{d_B}{d_W}} \tag{9}$$

and because the well width is smaller than the barrier width $d_W < d_B$, the 3D-power factor is here always smaller than the 2D-power factor.

$$\left(S^2_{W\&B}\sigma_{W\&B}\right)_{3D} < \left(S^2_W \sigma_W\right)_{2D} \tag{10}$$

E. g. for a well width d_W = 2 nm and a barrier width d_B = 30 nm in the system $Si/Si_{1-x}Ge_x$ the "only well" 2D-power factor $(S^2_W \sigma_W)_{2D}$ = 138.9 µW/(cmK²) and the "well & barrier" 3D-power factor $(S^2_{W\&B} \sigma_{W\&B})_{3D}$ = 8.7 µW/(cmK²) near room temperature. If the well width was changed from 4 nm to 1 nm $(S^2_W \sigma_W)_{2D}$ increases steady from 73.7 µW/(cmK²) to 201.0 µW/(cmK²), whereas $\left(S^2_{W\&B}\sigma_{W\&B}\right)_{3D}$ drops same in amount from 8.7 µW/(cmK²) to 6.5 µW/(cmK²). As explanation for this anti-running behavior the decreasing caused by interface scattering of the conductivity via the electron mobility with decreasing d_W is mentioned in [45].

To obtain thermoelectric film devices that use the advantages of the outstanding MQW-structure well properties in our opinion only an in-plane configuration (see Fig. 1) seems to be imagined. That means only the smaller, the most conservative estimation is given by eq. (9), 3D-power factor $\left(S^2_{W\&B}\sigma_{W\&B}\right)_{3D}$ will among other things directly determine the technical device parameters, because both the well and the barrier cross section have to be taken into the consideration. Under the aspect of device-application e. g. the n-type MQW-system $Si/Si_{1-x}Ge_x$ has a technical power factor $\left(S^2_{W\&B}\sigma_{W\&B}\right)_{3D}$ that lies in the same order as for sputtered 3D n-Bi_2Te_3 films (see Tab. 1 and Fig. 5) at room temperature. If we consider in addition, that the in-plane arrangement (see Fig. 1) is always connected with additionally (more or less) thermal losses by the parasitic heat flux through the required substrate it could be, that the excellence well transport properties using quantum confinement do not get an essential importance for the thermoelectric device parameters. Unfortunately is to notice that up to now questions concerning a thermoelectric MQW-device-design for a sensor, micro generator or micro cooler have not been stood in the focus of investigations.

Since a few years the theoretical and experimental investigations of low-dimensional systems have been also extended to 1D-systems as nanowires, nanowire arrays and segmented nanowires (see e. g. [48, 49]) and 0D-objects as quantum dots.

Nevertheless in point of view film device design the barriers (2D) or templates (1D) will causes always losses via a reduction of the 3D-power factor and by an additional thermal conductivity.

In our reflections above we have the term "superlattice" only associates with the physical effect of the quantum confinement of the charge carriers in the well of the MQW-structures by a change of the density of electronic states from 3D to 2D. But "superlattice"-structures are also connecting with the effect of the artificial reduction of the lattice thermal conductivity without a deterioration of the electronic material properties for a transport parallel to the growth direction. This phonon-blocking / electron-transmitting mechanism is described in [22] and represents quasi the Ioffe-concept on the nanoscale.

Objects, which show such properties, are samples with periodic heterostructures of different thermoelectric materials, deposited e. g. by molecular beam epitaxy (MBE) [50]. E. g. such a typical structure consists of alternating layers of Bi_2Te_3 and Sb_2Te_3 with thicknesses of a few nm. As main effect appears the large reduction (in the order of 2) of the phonon part of the thermal conductivity in the growth direction of the superlattice (SL) samples compared with the corresponding single bulk values without an accompanying decrease of the charge carrier mobilities. This phenomenon can be considered as a further beginning for the enhancement of the thermoelectric figure of merit Z (1) on a miniaturized level. This fact opens the possibility to use this effect for a device in the cross-plane configuration (see Fig. 2). First results to the investigations of such SL-samples operating in the cross-plane arrangement have been published for Bi_2Te_3-materials [22] and for Si/Ge-SL [51] with thicknesses of 5.2 µm and 120 nm, respectively. So in [51] a reduction of the thermal conductivity was observed up to the corresponding minimum value of amorphous Si.

To explain this effect, experimental and theoretical efforts have been made in the last years, see e. g. [52, 53]. It was found that several reasons are responsible for the reduction of the phonon thermal conductivity of SL-structures in the cross-plane configuration. So the influences of the appearance of more phonon branches in the reduced SL-Brillouin zone compared with the parent bulk materials, and mainly the sequential, diffuse phonon interface scattering are discussed for the interpretation. Nevertheless, it seems that a final explanation of this phenomenon is still outstanding.

Further, typical for the heat transport properties of SL-samples, is the fact that the thermal phonon conductivity is not only reduced in the SL-growth direction (cross-plane) but also in the plane perpendicular to this direction [50]. This opens the possibility to check out, whether the SL-structures can also be used for a favourable construction of in-plane devices. Of course, for an in-plane conception the parasitic heat flux through the substrate has to be taken into the consideration (see Fig. 1), whereas in the cross-plane configuration (see Fig. 2) the control of the enormous temperature gradients in the order of $(10^4 \ldots 10^5)$ Kcm^{-1} and of the high electrical and thermal contact resistances is a sophisticated technologically challenge.

Examples, Prototypes

Now we consider available examples of thin film devices all based on "normal" thermoelectric 3D-films. Fig. 8 shows a prototype of the 2nd generation developed by the German company D.T.S. GmbH (meanwhile the technology was moved from D.T.S. to the company angaris GmbH and the developments are there continued) using Bi_2Te_3-type material films deposited by sputtering including photolithography on a polyimid foil in an in-plane configuration.

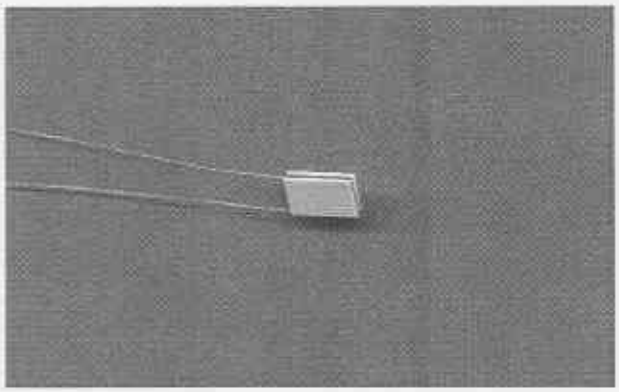

Fig. 8: Prototype (2nd generation) of a thermoelectric thin film generator developed by D.T.S.

Technical data of this prototype are given in Table 2.

Table 2: Technical data of the low power thermoelectric generator prototype shown in Fig. 8

Parameter	Unit	Value
geometrical		
total height	mm	1.8
length of base plate	mm	9.2
width of the base plate	mm	5.2
device volume	cm^3	0.084
number of thermocouples		5074
thermal		
thermal resistance	K/W	38
electrical at $\Delta T = 60$ K, matched load		
output power	µW	3030
resistance	kΩ	320
open circuit voltage	V	62.9
load voltage	V	31.5
current	µA	96.2

In comparison with the data of the 1st generation prototype published in [3, 4] together with the basic technology an essential improvement could be reached by the 2nd generation presented here. So e. g. for a temperature difference of 5 K the power output of the 1st prototype amounted 1.5 µW, whereas the recent device supplies 20 µW. This progress is schematically illustrated in Fig. 9. Main technological factors for the increase were the reduction of the internal resistance by using of thicker films (6 µm) and the reduction of the parasitic heat

flux by using of thinner (25 µm) substrate foils. With the tendency of a further miniaturization in addition the device volume and mass could be also distinctly reduced.

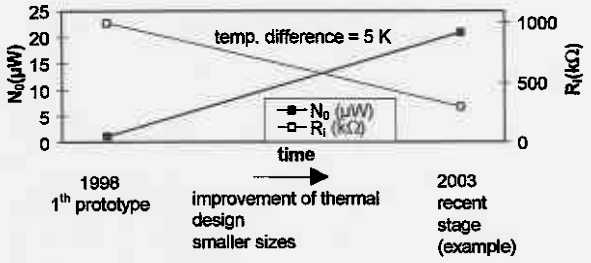

Fig. 9: Output power progress of thermoelectric thin film generators (see text)

In Figs. 10 and 11 an impression is given about the electrical behavior of this generator. Compared with a small reverse operated standard Peltier device an advantage of such thin film generators is the relatively high voltage already at relatively small temperature differences caused by the high number of thermocouples (see Table 2) connected in series. Therefore such thin film generators are especially suitable to convert body heat into usable electrical energy.

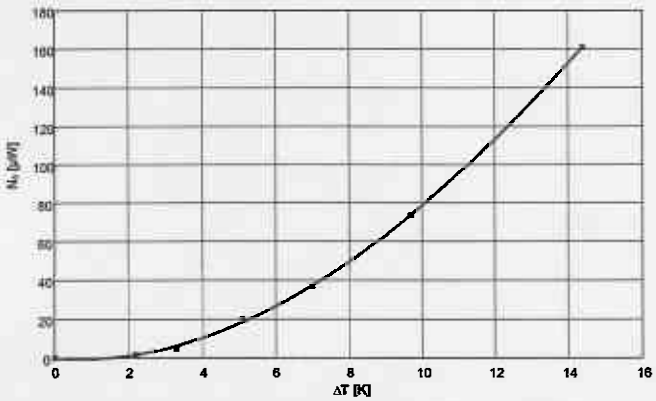

Fig. 10: Output power N_0 for small temperature differences ΔT for the thermoelectric generator shown in Fig. 8

An other kind of thin film generator is described in [14]. Here the thermopiles are formed by doped poly-Si and poly-$Si_{70}Ge_{30}$, respectively, using the established BiCMOS technology. The prototype arrangement is demonstrated in Fig. 12.
A feature of this type of generator is, that the heat flux goes vertical through the chip and generates the usable temperature differences in the plane perpendicular to the heat flux at the p-n-junctions. Therefore the output power is scalable and proportional to the device surface. For an area of 1 cm^2 the output power in dependence of the temperature difference is given in Fig. 13 after [54].

The relatively high electrical resistance of the thermocouples here mainly limits the output power. So the entire resistance amounts 205 Ω and 639 Ω for a poly-Si and poly-SiGe [14] thermopile, respectively. The comparable value for the generator given in Fig. 8 is 63 Ω (see Table 2).

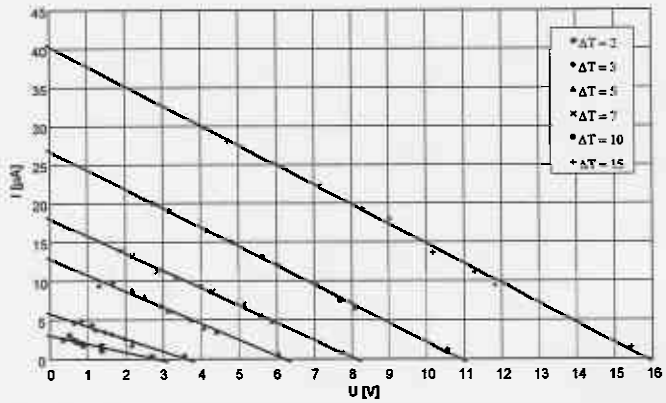

Fig. 11: Current (I)-voltage (U)-plot at six small temperature differences ΔT for the thermoelectric generator shown in Fig. 8

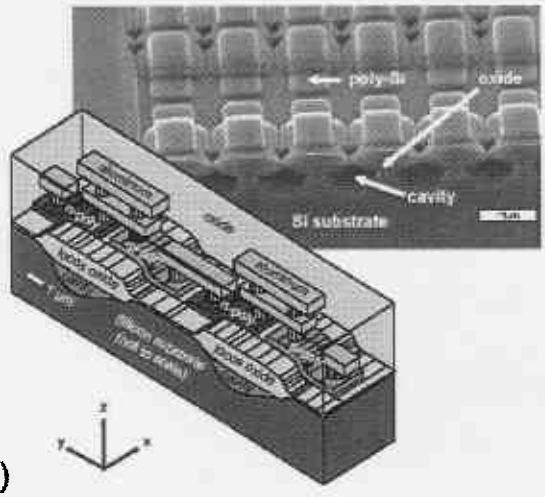

Fig. 12: Schematic view of two thermoelectric couples of the BiCMOS realization at infineon after [14]. The heat flow is here in the vertical (z) direction and generates temperature differences at the p-n-junctions in the (x,y)-plane.
The photo shows the etched cavities.

Predominantly under the aspect to construct a miniaturized Peltier cooling element especially for applications in the telecommunication sector, in Germany at the IPM FhG was developed such a device [5, 17, 55]. For the assembly of this component the "classic" cross-plane configuration was chosen and is illustrated in Fig. 14. The film legs have a thickness of about 20 µm and for p- and n-type the materials $(Bi,Sb)_2Te_3$ and Bi_2Te_3 were used, respectively. The films were deposited also by sputtering technology and the pattern generation was carried out by an especially dry etch techniques.
Detailed data of the small Peltier device we can find in [55].

Of course this element can also operate in the Seebeck mode to generate electrical energy. For this case the power

output versus the temperature difference is demonstrated after [55] in Fig. 15.

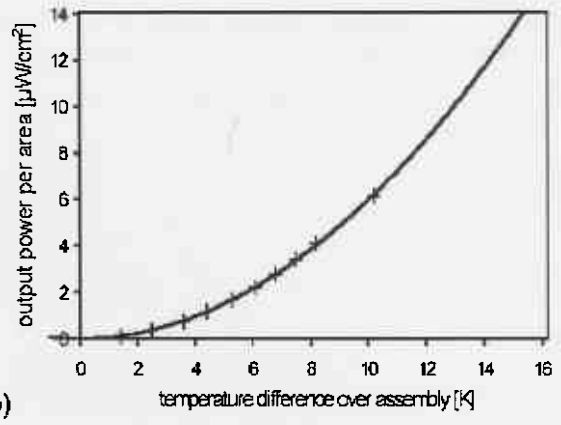

Fig. 13: Output power in dependence of the temperature difference of the generator based on poly-Si films (see Fig. 12 and text) after [54]

Certainly a direct comparison between the selected and here as examples mentioned thin film devices seems not possible and not meaningful, because the device concepts and applications are to different from each other. On the other hand these discussed prototypes are representative to characterize the recent technological level especially for the miniaturized thermoelectric thin film generators.

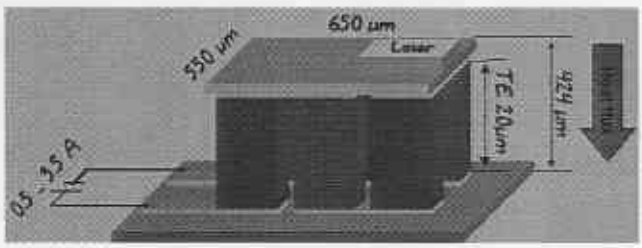

Dimensions (mm)

Cold side : 0.65 X 0.5
Hot side : 1.50 X 0.90
Thickness : 0.424

Fig. 14: Schematic drawing of a possible telecommunication cooler device after [5]

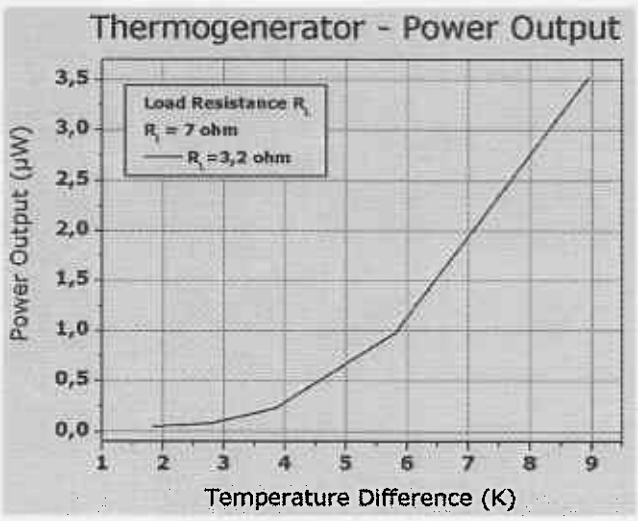

Fig. 15: Power output of the „micropelt" device (IPM FhG) operating in the Seebeck mode after [55]

Summary

Thin film thermoelectric devices are sensors, self-powered energy sources (generators) or Peltier coolers in a miniaturized form for low power applications.

Besides true electronic stand-alone solutions using mainly waste heat, the conversion of body heat into electrical energy opens a wide market segment for battery less monitoring of humans and animals.

Thin film thermoelectric generators and coolers are developed in the prototype stage and at the present time still not commercial available on the market.

Target of the international development efforts is the enhancement of the power factor and the figure-of-merit of the thermoelectric thin film materials.

Whereas the power factor of p-Bi_2Te_3-material thin films is near the corresponding bulk values, the power factor enhancement of the n-Bi_2Te_3-type films is a currently task of prime importance to improve the efficiency of the devices operating in the in-plane or cross-plane configuration.

The reduction of the electrical and thermal contact resistances especially in the cross-plane and the use of thinner substrates in the in-plane configuration are technologically challenges for the increase of the thin film device efficiency.

For the estimation of the potential of thermoelectric structures operating after the principles of quantum confinement (multiple quantum wells) and phonon-blocking / electron-transmitting (superlattices) it would be useful to have more detailed device concepts.

Acknowledgement

We thank Dr. J. Schumann (IFW Dresden) for the support of the high temperature measurements (see Figs. 4 and 5) and the CEO of angaris, Mr. Bernd Engers, for his supporting interest in the subject.

References

1. D. M. Rowe (Ed.), Handbook of Thermoelectrics, CRC Press Boca Raton, New York, London, Tokyo, (1995).
2. V. A. Semenyuk, "Advances in Development of Thermoelectric Modules for Cooling Electro-Optic Components", *Proc. 22nd ICT '03*, La Grande-Motte (2003) 631.
3. M. Stordeur and I. Stark, "Low Power Thermoelectric Generator – self-sufficient energy supply for micro systems", *Proc. 16th ICT '97*, Dresden (1997) 575.
4. I. Stark and M. Stordeur, "New Micro thermoelectric Devices Based on Bismuth Telluride-Type Thin Solids Films", *Proc. 18th ICT '99*, Baltimore, MD (1999) 465.
5. H. Böttner, A. Schubert, K. H. Schlereth, D. Eberhard, A. Gavrikov, M. Jägle, G. Kühner, C. Künzel, J. Nurnus, and G. Plescher, "New Thermoelectric Components using Micro-System-Technologies", *Proc. 6th European Workshop on Thermoelectrics,* Freiburg i. B. (2001).

6. M. Stölzer, V. Bechstein, and J. Meusel, "Crystalline structure and thermoelectric properties versus growing conditions of sputtering-deposited $(Bi_{1-x}Sb_x)_2Te_3$ films with $0 \leq x \leq 0.85$", *Proc. 16th ICT '97*, Dresden (1997) 93.
7. J.-P. Fleurial, G. J. Snyder, J. A. Herman, P. H. Giauque, W. M. Phillips, M. A. Ryan, P. Shakkottai, E. A. Kolaw, and M. A. Nicolet, "Thick-Film Thermoelectric Microdevices", *Proc. 18th ICT '99*, Baltimore, MD (1999) 294.
8. J. R. Lim, G. J. Snyder, C.-K. Huang, J. A. Herman, M. A. Ryan, and J.-P. Fleurial, "Thermoelectric Microdevice Fabrication Process and Evaluation at the Jet Propulsion Laboratory (JPL)", *Proc. 21st ICT '02*, Long Beach CA (2002) 535.
9. S. Diliberto, S. Michel, C. Boulanger, J. M. Lecuire, M. Jägle, S. Drost, and H. Böttner, "A technology for a device prototyping based on electrodeposited thermoelectric V-VI layers," *Proc. 22nd ICT '03*, La Grande-Motte (2003) 661.
10. M. O. Boffoué, A. Dauscher. B. Lenoir, A. Jacquot, H. Scherrer, J. Meusel, M. Stölzer, "Preparation of Bi thin films by pulser laser deposition – transport properties", *Proc. 5th European Workshop on Thermoelectrics*, Pardubice-Lázně Bohdaneč (1999) 47.
11. R. Zeipl, S. Karamazov, M. Jelínek, P. Lošťák, M. Pavelka, Sz. Winiarz, R. Czajka, J. Vaniš, F. Šroubek, J. Zelinka, and J. Walachová, "Very Thin Layers Prepared By Laser Ablation From Bi_2Te_3 Target", *Proc. 22nd ICT '03*, La Grande-Motte (2003) 342.
12. L. W. da Silva, M. Kaviany, A. DeHennis, and J. S. Dyck, "Micro Thermoelectric Cooler Fabrication: Growth and Characterization of Patterned Sb_2Te_3 and Bi_2Te_3 Films", *Proc. 22nd ICT '03*, La Grande-Motte (2003) 665.
13. K. Miyazaki, T. Iida, and H. Tsukamoto, "Microfabrication of Bi_2Te_3 by Using Micro-jet", *Proc. 22nd ICT '03*, La Grande-Motte (2003) 641.
14. M. Strasser, R. Aigner, and G. Wachutka, "Microscale BiCMOS Thermoelectric Generators Based on Surface Micromachining", *Proc. 6th European Workshop on Thermoelectrics*, Freiburg i. B. (2001).
15. M. Ashauer, H. Golsch, F. Hedrich, N. Hey, H. Sandmaier, and W. Lang, "Thermal Flow Sensors for Liquids and Gases", *Proc. 2. 9th Int'l Trade Fair and Conference for Sensors Transducer & Systems*, Nürnberg (1999) 387.
16. G. Min and D. M. Rowe, "Recent Concepts in Thermoelectric Power Generation", *Proc. 21st ICT '02*, Long Beach CA (2002) 365.
17. H. Böttner, "Thermoelectric Micro Devices: Current State, Recent Developments and Future Aspects for Technological Progress and Applications", *Proc. 21st ICT '02*, Long Beach CA (2002) 511.
18. I. H. Kim and D. H. Lee, "Thin Film Thermoelectric Generator Cell of Bi-Sb-Te-Se System", *Proc. 15th ICT '96*, Pasadena CA (1996) 425.
19. L. D. Hicks and M. S. Dresselhaus, "Effect of quantum-well structures on the thermoelectric figure of merit", *Phys. Rev. B*, Vol. 47, No. 19, (1993) 12727.
20. D. G. Mahan and H. B. Lyon, "Thermoelectric devices using semiconductor quantum wells", *J. Appl. Phys.*, Vol. 76 No. 3, (1994) 1899.
21. M. S. Dresselhaus, T. Koga, X. Sun, S. B. Cronin, K. L. Wang, and G. Chen, "Low Dimensional Thermoelectrics", *Proc. 16th ICT '97*, Dresden (1997) 12.
22. R. Venkatasubramanian, E. Silivola, T. Colpitts, and B. O'Quinn, "Thin-film thermoelectric devices with high room-temperature figures of merit", *Nature*, Vol. 413, (2001) 597.
23. A. S. Kushch, J. C. Bass, S. Ghamaty, and N. B. Elsner, "Thermoelectric Development at Hi-Z Technology", *Proc. 20th ICT '01*, Beijing (2001) 422.
24. A. Jacquot, W. L. Liu, J.-P. Fleurial, A. Dauscher, and B. Lenoir, "Fabrication and modeling of an in-plane thermoelectric micro-generator", *Proc. 21st ICT '02*, Long Beach CA (2002) 561.
25. E. Kessler, U. Dillner, V. Baier, and J. Müller, "A 256 pixel linear thermopile array using materials with high thermoelectric efficiency", *Proc. 16th ICT '97*, Dresden (1997) 734.
26. T. Elbel, M. Bethke, M. Rahf, D. Runge, W. Schuppe, and E. Kessler, "Smart Micro Gas Flow Sensors with a Thinfilm Thermopile", *Proc. 1. 9th Int'l Trade Fair and Conference for Sensors Transducer & Systems*, Nürnberg (1999) 225.
27. J. Schumann, "Thermoelectric Sensors and Transducers", Metal Based Thin Films for Electronics, K. Wetzig and C. M. Scheider (eds.), WILEY-VCH Weinheim (2003) 349.
28. H. Böttner, M. Jaegle, Ch. Künzel, M. Benkendorf. U. Vetter, P. Auer, and A. Lambrecht, "Nanocalorimetric Devices with Thermoelectric PECVD p-Si_{1-x} Ge_x Thin Film Layers for the Analysis of Bioglogical Phase Transitions", *Proc. 22nd ICT '03*, La Grande-Motte (2003) 669.
29. M. Stordeur and I. Stark, "Thermoelectric Sensor for hf-Power Detection", *Proc. 6th European Workshop on Thermoelectrics*, Freiburg i. B. (2001).
30. M. H. Cobble, "Calculations of Generator Performance", Handbook of Thermoelectrics, D. M. Rowe (Ed.), CRC Press Boca Raton, New York, London, Tokyo, (1995) 489.
31. H. H. Saber and M. S. El-Genk, "Optimization of Segmented Thermoelectric for Maximizing Conversion Efficiency and Electric Power Density", *Proc. 21st ICT '02*, Long Beach CA (2002) 404.
32. M. Stordeur, "Valence Band Structure and the Thermoelectric Figure-of-Merit of $(Bi_{1-x}Sb_x)_2Te_3$ Crystals", Handbook of Thermoelectrics, D. M. Rowe (Ed.), CRC Press Boca Raton, New York, London, Tokyo, (1995) 239.
33. T. Ohata and T. Kajikawa, "PIES Method of Preparing Bismuth Alloys", Handbook of Thermoelectrics, D. M. Rowe (Ed.), CRC Press Boca Raton, New York, London, Tokyo, (1995) 109.
34. T. Tokiai, T. Uesugi, and Y. Yoneyama, " High Perform Thermoelectric Properties of (Bi_2Te_3), (Sb_2Te_3) System with PIES Powder by HIP Treatment", *Proc. 12th ICT '93*, Yokohama (1993) 281.
35. J.-M. Simard, D. Vasilevskiy, F. Belanger, J. L'Ecuyer, and S. Turenne, "Production of thermoelectric Materials by Mechanical Alloying - Extrusion Process", *Proc. 20th ICT '01*, Beijing (2001) 132.

36. H. Zou, D. M. Rowe, and S. G. K. Williams, "Peltier effect in a co-evaporated Sb_2Te_3(P)-Bi_2Te_3(N) thin film thermocouple", *Thin Solid Films,* Vol. 408 (2002) 270.
37. T. E. Svechnikova and N. M. Maksimova, "Electrophysical properties of $Bi_2Te_{2.85}Se_{0.15}$ single crystals doped with copper", *Proc. 16th ICT '97*, Dresden (1997) 109.
38. K. Nakamura, K. Morikawa, H. Owada, K. Miura, K. Ogawa, and I. A. Nishida, "Thermoelectric Properties of n-type $Bi_2Te_{2.85}Se_{0.15}$ Prepared by Pressing and Sintering", *Proc. 12th ICT '93*, Yokohama (1993) 110.
39. H. T. Kaibe, M. Sakata, and I. A. Nishida, "Thermoelectric Cooling Properties of the π-shaped Thermocouples Consisting of the Sintered Bi_2Te_3 and Sb_2Te_3 Based Compounds", *Proc. 12th ICT '93*, Yokohama (1993) 165.
40. W. Brode, K. Bruehne, M. Rakhlin, M. Schubert, T. Pannek, H. Beyer, D. Eberhard, C. Künzel, A. Lambrecht, I. Stark, M. Stordeur, G. Paul, V. Sauchuk, and J. Schumann, "Development of Thermoelectrical Material Systems for Thin Film Sensor and Generator Devices", *Proc. 6th European Workshop on Thermoelectrics,* Freiburg i. B. (2001).
41. T. Takashiri, T. Borca-Tasciuc, O. Olubuyide, A. Jacquot, J. Hoyt, and G. Chen, "Transport Porperties of Polycristalline $Si_{0.8}Ge_{0.2}$ Thin Films for Micro Power Generators", *Proc. 22nd ICT '03*, La Grande-Motte (2003) 395.
42. T. L. Reinecke and D. A. Broido, "Thermoelectric Transport in Low Dimensional Superlattice Systems", *Proc. 16th ICT '97,* Dresden (1997) 424.
43. T. C. Harman, D. L. Spears, D. R. Calawa, S. H. Groves, and M. P. Walsh, "Characterization of p-type PbEuTe/PbTe MQW Structures with High Thermoelectric Figures of Merit in the PbTe Quantum Wells", *Proc. 16th ICT '97,* Dresden (1997) 416.
44. I. Sur, A. Casian, A, A. Balandin, and Z. Dashevsky, "Thermoelectric Properties of p-type PbTe/PbEuTe Quantum Well Structures", *Proc. 22nd ICT '03*, La Grande-Motte (2003) 403.
45. X. Sun, S. B. Cornin, J. Liu, K. L. Wang, T. Koga, M. S. Dresselhaus, and G. Chen, "Experimental Study of the Effect of the Quantum Well Structures on the Thermoelectric Figure of Merit in $Si/Si_{1-x}Ge_x$ System", *Proc. 18th ICT '99*, Baltimore, MD (1999) 652.
46. H. Beyer, A. Lambrecht, J. Nurnus, H. Böttner, H. Griessmann, A. Heinrich, L. Schmitt, M. Blumers, and F. Völklein, "Thermoelectric Properties of Epitaxial PbSrTe and PbSrSe Bulk and MQW Thin Films", *Proc. 18th ICT '99*, Baltimore, MD (1999) 687.
47. S. V. Melnichuk, S. V. Kosyachenko, and M. V. Vozny, " Thermoelectric properties of superlattices", *Proc. 16th ICT '97,* Dresden (1997) 438.
48. Yu-M. Lin, O. Rabin, and M. S. Dresselhaus, "Segmented Nanowires: a theoretical study of thermoelectric properties", *Proc. 21st ICT '02*, Long Beach CA (2002) 265.
49. W. Wang, F. Ila, J. Zhu, and J. Zhang, "A New Type of Micro-thermoelectric Power Generator Fabricated By Nanowire Array Thermoelectric Material", *Proc. 22nd ICT '03*, La Grande-Motte (2003) 682.
50. A. Lambrecht, H. Bever, J. Nurnus, C. Künzel, and H. Böttner, "High Figure of Merit ZT in PbTe and Bi_2Te_3 Based Superlattice Structures by Thermal Conductivity Reduction", *Proc. 20th ICT '01,* Beijing (2001) 335.
51. B. Yang, J. Liu, K. Wang, and G. Chen, "Characterization of Cross-Plane Thermoelectric Properties of Si/Ge Superlattices", *Proc. 20th ICT '01,* Beijing (2001) 344.
52. G. Chen, B. Yang, W. L. Liu, T. Borca-Tasciuc, D. Song, D. Achimov, M. S. Dresselhaus, J. L. Liu, and K. Wang, "Thermoelectric Property Characterization of Low Dimensional Structures", *Proc. 20th ICT '01,* Beijing (2001) 30.
53. G. Chen, C. Dames, T. Harris, D. Borca-Tasiuc, R. G. Yang, B. Yang, W. L. Liu, D. Song, and M. Takashiri, "Thermal Conductivity Reduction Mechanisms in Superlattices", *Proc. 22nd ICT '03*, La Grande-Motte (2003) 336.
54. W. Weber, R. Glaser, S. Jung, C. Lauterbach, G. Stromberg, and T. Sturm, "Electronics in Textiles – The next Stage in Man Machine Interaction", www.infineon.de (2003).
55. www.micropelt.com (2004)